SAGA-HE-196-03 (hep-ph/0307105) June 30, 2003

Nuclear modification of structure functions in lepton scattering

S. Kumano *

Department of Physics
Saga University
Saga, 840-8502, Japan

Talk at the Second International Workshop on
Neutrino-Nucleus Interactions in the Few GeV Region

UC Irvine, USA, December 12 - 15, 2002

(talk on Dec. 13, 2002)

* Email: kumanos@cc.saga-u.ac.jp. URL: http://hs.phys.saga-u.ac.jp.

to be published in Nucl. Phys. B Supplements

Nuclear modification of structure functions in lepton scattering

S. Kumano [a] *

[a]Department of Physics, Saga University, Saga, 840-8502, Japan

We discuss nuclear structure functions in lepton scattering including neutrino reactions. First, the determination of nuclear parton distribution functions is explained by using the data of electron and muon deep inelastic scattering and those of Drell-Yan processes. Second, NuTeV $sin^2\theta_W$ anomaly is discussed by focusing on nuclear corrections in the iron target. Third, we show that the HERMES effect, which indicates nuclear modification of the longitudinal-transverse structure function ratio, should exist at large x with small Q^2 in spite of recent experimental denials at small x.

1. Introduction

Modification of nuclear structure functions or nuclear parton distribution functions (NPDFs) is known especially in electron and muon scattering. In neutrino scattering, such nuclear effects have not been seriously investigated due to the lack of accurate deuteron data. Nuclear effects in the PDFs have been investigated mainly among hadron structure physicists. However, demands for accurate NPDFs have been growing from other fields in the recent years. In fact, one of the major purposes of this workshop [1] is to describe neutrino-nucleus cross sections for long baseline neutrino experiments, so that neutrino oscillations could be understood accurately [2,3].

In the near future, neutrino cross sections should be understood within a few percent level for the oscillation studies [2,3]. Because typical nuclear corrections in the oxygen nucleus are larger than this level, they should be precisely calculated. In low-energy scattering, the nuclear medium effects are discussed in connection with nuclear binding, Fermi motion, short-range correlations, Pauli exclusion effects, and other nuclear phenomena. In this paper, the nuclear corrections are discussed in the structure functions and the PDFs by focusing on the high-energy region. These studies are important not only for the neutrino studies but also for other applications. For example, they are used in heavy-ion physics [4] for understanding accurate initial conditions of heavy nuclei, so that one could make a definitive statement, for example on quark-gluon plasma formation, in the final state. They could be also used in understanding nuclear shadowing mechanisms [5].

In this paper, recent studies are explained on the nuclear effects which are relevant to high-energy neutrino scattering. First, a recent NPDF χ^2 analysis is reported. Although the unpolarized PDFs in the nucleon have been investigated extensively [6], the NPDFs are not well studied. However, there are some studies to obtain optimum NPDFs by using a simple parametrization form and nuclear scattering data [7,8]. We explain the current situation. Second, NuTeV $sin^2\theta_W$ anomaly [9] is investigated in a conservative way, namely in terms of nuclear corrections [10–13]. The NuTeV collaboration obtained anomalously large $sin^2\theta_W$. Before discussing any new physics mechanisms [14], we should exclude possible nuclear physics explanations. In particular, the used target is the iron and it may cause complicated nuclear medium effects. Third, the HERMES effect [15], which is nuclear modification of the longitudinal-transverse structure function ratio, is investigated in a simple convolution model. It is intended to show that such an effect should exist in the medium and large x regions [16] in spite of recent experimental denials at small x [17,18]. In particular, the nucleon Fermi motion in a nucleus could play an impor-

*kumanos@cc.saga-u.ac.jp, http://hs.phys.saga-u.ac.jp

tant role for the nuclear modification.

This paper consists of the following. In section 2, global NPDF analysis results are shown The $sin^2\theta_W$ anomaly topic is discussed in section 3. The HERMES effect is explained in section 4. The results are summarized in section 5.

2. Nuclear parton distribution functions

The determination of the NPDFs is not still satisfactory in comparison with the one for the nucleon. It is partly because enough data are not obtained for fixing each distribution from small x to large x. For example, various scaling violation data are not available, unlike the HERA data for the proton, at very small x for fixing gluon distributions. However, the determination of nuclear PDFs has been awaited for describing high-energy nuclear scattering phenomena, including neutrino-nucleus and heavy-ion reactions. Some efforts have been made to provide practical parametrizations for the NPDFs, such as the ones by Eskola, Kolhinen, Ruuskanen, Salgado [7] and the ones by the HKM analysis [8]. In the following, the NPDFs are discussed based on the latter study in Ref. [8].

First, the parametrization form should be selected. From the studies of nuclear F_2 structure function ratios F_2^A/F_2^D, one knows the existence of shadowing phenomena at small x, antishadowing at $x \approx 0.2$, depletion at medium x, and then a positive nuclear modification at large x. In order to express such x dependence, the following functions are used for the initial NPDFs at Q_0^2=1 GeV^2:

$$f_i^A(x,Q_0^2) = w_i(x,A,Z)\, f_i(x,Q_0^2),$$
$$w_i(x,A,Z) = 1 + \left(1 - \frac{1}{A^{1/3}}\right) \times \frac{a_i(A,Z) + b_i x + c_i x^2 + d_i x^3}{(1-x)^{\beta_i}}. \quad (1)$$

Here, Z is the atomic number, A is the mass number, and the subscript i indicates a distribution type: i=u_v, d_v, $\bar{q}$, or g. The functions f_i^A and f_i are the PDFs in a nucleus and the nucleon, respectively, so that the weight function w_i indicates nuclear medium effects. The nuclear modification $w_i - 1$ is assumed to be proportional to $1 - 1/A^{1/3}$, and its x dependence is taken to be a cubic functional form with the $1/(1-x)^{\beta_i}$ factor for describing the Fermi-motion part. The parameters a_i, b_i, c_i, and d_i are determined by a χ^2 analysis of experimental data.

Although the flavor dependence of the antiquark distributions is known in the nucleon [19], the details of nuclear antiquark distributions cannot be investigated at this stage. Therefore, flavor symmetric antiquark distributions are assumed in the parametrization.

The electron and muon deep inelastic experimental data and Drell-Yan data are fitted by the NPDFs in Eq. (1). The initial NPDFs are, of course, evolved to various experimental Q^2 points, and χ^2 values are calculated in comparison with the data for electron and muon deep inelastic scattering and Drell-Yan processes:

$$\chi^2 = \sum_j \frac{(R_j^{data} - R_j^{theo})^2}{(\sigma_j^{data})^2}. \quad (2)$$

Here, R is the ratio $F_2^A/F_2^{A'}$ or $\sigma_{DY}^A/\sigma_{DY}^{A'}$. These structure functions and the DY cross sections are calculated in the leading order. The experimental error is given by systematic and statistical errors as $(\sigma_j^{data})^2 = (\sigma_j^{sys})^2 + (\sigma_j^{stat})^2$. The first version was published in 2001, and then the research is in progress by including the Drell-Yan data. We discuss the obtained NPDFs by these analyses.

Obtained optimum distributions are shown for the calcium nucleus at Q^2=1 GeV^2 in Fig. 1. The solid, dashed, and dotted curves indicate the weight functions for the valence-quark, antiquark, and gluon distributions. The valence distribution is well determined in the medium x region, but it is difficult to determine it at small x although it is constrained by the baryon-number and charge conservations. In fact, it will be one of the NuMI projects [20] to determine the valence-quark (F_3) shadowing in comparison with the antiquark (F_2) shadowing by neutrino-nucleus scattering. On the other hand, the antiquark distribution is well determined at small x; however, it cannot be fixed at medium x ($x > 0.2$) in spite of the momentum-conservation constraint. Because this is the leading order analysis, the gluon distribution is not

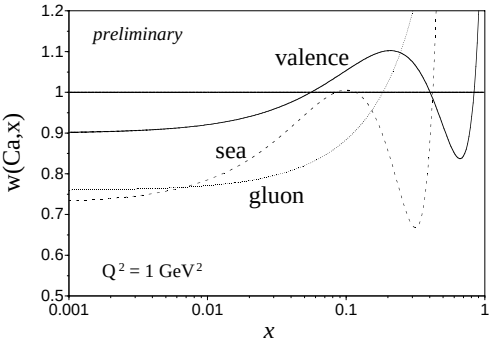

Figure 1. Obtained weight functions for the calcium nucleus at Q^2=1 GeV^2.

fixed in the whole x region.

The obtained NPDFs are available at the web site http://hs.phys.saga-u.ac.jp/nuclp.html, where computer codes are available for calculating the distributions at given x and Q^2 for a requested nucleus. The nuclear type should be in the range, $2 \leq A \leq 208$, in principle, because the analyzed nuclei are in this range. However, the distributions could be also calculated for larger nuclei ($A > 208$) because variations of the NPDFs are rather small in such a large-A region. If one wishes to use an analytical form, the distributions at Q^2=1 GeV^2 are provided in the appendix of Ref. [8]. After the first version was published, a new analysis has been investigated. The second version will become available within the year of 2003.

3. A nuclear physicist's view of $sin^2\theta_W$ anomaly

The NuTeV collaboration announced that their measurement of the weak mixing angle $sin^2\theta_W$ is significantly different from collider measurements. If the neutrino-nucleus scattering data are excluded, a global analysis indicates $sin^2\theta_W^{on-shell} = 0.2227 \pm 0.0004$ [21]. On the other hand, the NuTeV reported [9]

$$sin^2\theta_W = 0.2277 \pm 0.0013\,(\mathrm{stat}) \pm 0.0009\,(\mathrm{syst})\,, \tag{3}$$

by using their neutrino and antineutrino scattering data.

Because it is one of the important constants in the standard model, we should find a reason for the discrepancy. Although it may indicate the existence of a new mechanism [14], we should seek a conservative explanation first. In particular, the NuTeV target is the iron nucleus so that nuclear medium effects might have altered the $sin^2\theta_W$ value [10–13]. In the following, we explain nuclear effects on the $sin^2\theta_W$ determination.

The neutrino and antineutrino cross section data are analyzed by a special Monte Carlo code, so that it is not theoretically straightforward to investigate a possible explanation. In order to simplify the investigation, we study nuclear effects on the Paschos-Wolfenstein (PW) relation, which is considered to be "implicitly" used in the NuTeV analysis. The PW relation [22] is given by the ratio of charged current (CC) and neutral current (NC) cross sections:

$$R^- = \frac{\sigma_{NC}^{\nu N} - \sigma_{NC}^{\bar{\nu} N}}{\sigma_{CC}^{\nu N} - \sigma_{CC}^{\bar{\nu} N}} = \frac{1}{2} - sin^2\theta_W\,. \tag{4}$$

This relation is valid for the isoscalar nucleon; however, corrections should be carefully investigated for the non-isoscalar iron target.

If the relation is calculated for a nucleus in the leading order of α_s, we obtain [12]

$$\begin{aligned} R_A^- &= \frac{\sigma_{NC}^{\nu A} - \sigma_{NC}^{\bar{\nu} A}}{\sigma_{CC}^{\nu A} - \sigma_{CC}^{\bar{\nu} A}} \\ &= \{1-(1-y)^2\}\,[\,(u_L^2 - u_R^2)\{u_v^A(x) + c_v^A(x)\} \\ &\qquad + (d_L^2 - d_R^2)\{d_v^A(x) + s_v^A(x)\}\,] \\ &\quad /\,[\,d_v^A(x) + s_v^A(x) - (1-y)^2\,\{u_v^A(x) + c_v^A(x)\}\,]\,, \end{aligned} \tag{5}$$

where the valence quark distributions are defined by $q_v^A \equiv q^A - \bar{q}^A$. The couplings are expressed by the weak mixing angle as $u_L = 1/2 - (2/3)\,sin^2\theta_W$, $u_R = -(2/3)\,sin^2\theta_W$, $d_L = -1/2 + (1/3)\,sin^2\theta_W$, and $d_R = (1/3)\,sin^2\theta_W$. It is known that the nuclear distributions are modified from those for the nucleon. The modification for u_v^A and d_v^A could be expressed by the weight

functions w_{u_v} and w_{d_v} at any Q^2:

$$u_v^A(x) = w_{u_v}(x,A,Z)\,\frac{Z\,u_v(x)+N\,d_v(x)}{A},$$
$$d_v^A(x) = w_{d_v}(x,A,Z)\,\frac{Z\,d_v(x)+N\,u_v(x)}{A}, \quad (6)$$

although w_i in section 2 is defined at fixed Q^2 ($=Q_0^2$). Here, u_v and d_v are the distributions in the proton, and N is the neutron number.

In order to find possible deviation from the PW relation, we first define a function which is related to the neutron excess in a nucleus: $\varepsilon_n(x) = [(N-Z)/A](u_v-d_v)/(u_v+d_v)$, and then a difference between the weight functions is defined by

$$\varepsilon_v(x) = \frac{w_{d_v}(x,A,Z) - w_{u_v}(x,A,Z)}{w_{d_v}(x,A,Z) + w_{u_v}(x,A,Z)}\,. \quad (7)$$

Furthermore, there are correction factors associated with the strange and charm quark distributions, so that we define ε_s and ε_c by $\varepsilon_s = s_v^A/[w_v\,(u_v+d_v)]$ and $\varepsilon_c = c_v^A/[w_v\,(u_v+d_v)]$ with $w_v = (w_{d_v}+w_{u_v})/2$.

Neutron-excess effects are taken into account in the NuTeV analysis as explained by McFarland *et al.* [10], and they are also investigated by Kulagin [13]. The strange quark (ε_s) contribution is small according to Zeller *et al.* [23], and it increases the deviation. Here, we investigate a different contribution from the $\varepsilon_v(x)$ term [12]. Writing Eq. (5) in terms of the factors, ε_n, ε_v, ε_s, and ε_c, and then expanding the expressions by these small factors, we obtain

$$R_A^- = \frac{1}{2} - sin^2\theta_W$$
$$-\,\varepsilon_v(x)\left\{\left(\frac{1}{2}-sin^2\theta_W\right)\frac{1+(1-y)^2}{1-(1-y)^2} - \frac{1}{3}sin^2\theta_W\right\}$$
$$+\,O(\varepsilon_v^2) + O(\varepsilon_n) + O(\varepsilon_s) + O(\varepsilon_c)\,. \quad (8)$$

Because only the ε_v contribution is discussed in the following, other terms are not explicitly written in the above equation. This equation indicates that the observed $sin^2\theta_W$ in neutrino-nucleus scattering is effectively larger if the ratio is calculated without the ε_v correction.

The nuclear modification difference $\varepsilon_v(x)$ is not known at all at this stage. We try to estimate it theoretically by using charge and baryon-number conservations: $Z = \int dx\,A\sum_q e_q(q^A-\bar{q}^A)$ and $A = \int dx\,A\sum_q(1/3)\,(q^A-\bar{q}^A)$. These equations are expressed by the valence-quark distributions, then they becomes

$$\int dx\,(u_v+d_v)\,[\,\Delta w_v + w_v\,\varepsilon_v(x)\,\varepsilon_n(x)\,] = 0\,, \quad (9)$$

$$\int dx\,(u_v+d_v)\,[\,\Delta w_v\,\{1-3\,\varepsilon_n(x)\}$$
$$-\,w_v\,\varepsilon_v(x)\,\{3-\varepsilon_n(x)\}\,] = 0\,, \quad (10)$$

where Δw_v is defined by $\Delta w_v = w_v - 1$. These equations suggest that there should exist a finite distribution for $\varepsilon_v(x)$ due to the charge and baryon-number conservations. However, there is no unique solution for these integral equations, so that the following discussions become inevitably model dependent.

We provide two examples for estimating the order of magnitude of the effect on $sin^2\theta_W$. First, the integrands of Eqs. (9) and (10) are assumed to vanish by neglecting the higher-order terms $O(\varepsilon_v\varepsilon_n)$:

$$\text{case 1:}\;\; \varepsilon_v(x) = -\varepsilon_n(x)\,\frac{\Delta w_v(x)}{w_v(x)}\,. \quad (11)$$

Second, the χ^2 analysis result [8], which is explained in section 2, could be used for the estimation:

$$\text{case 2:}\;\; \varepsilon_v(x) = \left[\frac{w_{d_v}(x)-w_{u_v}(x)}{w_{d_v}(x)+w_{u_v}(x)}\right]_{\chi^2\ \text{analysis}}\,. \quad (12)$$

These two descriptions are numerically estimated and the results are shown at Q^2=20 GeV^2 in Fig. 2. The solid and dashes curves indicate the case 1 and 2, respectively.

In the first case, the function ε_v is directly proportional to the nuclear modification $\Delta w_v(x)$, so that it changes the sign at $x \sim 0.2$. In comparison with the NuTeV deviation 0.005, which is shown by the dotted line, $\varepsilon_v^{(1)}$ is of the same order of magnitude. On the other hand, the second one $\varepsilon_v^{(2)}$ is rather small. This is partly because of the assumed functional form in the χ^2 analysis [8], which was not intended especially to obtain the

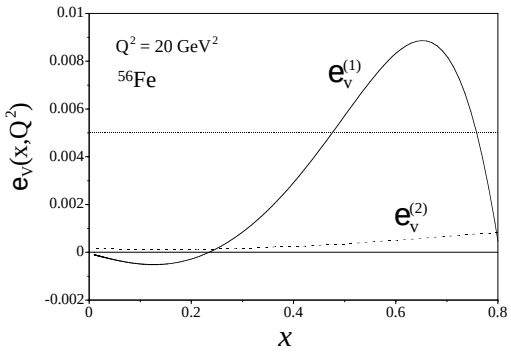

Figure 2. The function $\varepsilon_v(x, Q^2)$ is estimated by two different descriptions at Q^2=20 GeV^2.

nuclear modification difference ε_v. Because the distributions are much different depending on the model, numerical estimates are merely considered to be an order of magnitude estimate.

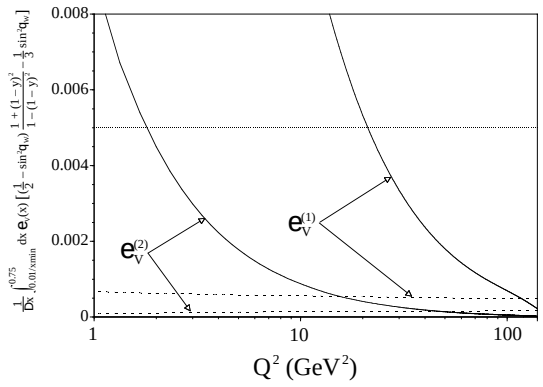

Figure 3. Contributions to $sin^2\theta_W$ are calculated by taking the x average and they are shown by the solid curves. The dashed curves are calculated by taking the NuTeV kinematics into account [12].

As far as we see Fig. 2, our mechanism seems to a promising explanation for the NuTeV anomaly. If a simple x average is taken for the ε_v contribution to the $sin^2\theta_W$ determination, we obtain the solid curves in Fig. 3, and they are of the order of the NuTeV deviation. However, the situation is not so simple. Although the function $\varepsilon_v^{(1)}$ is large in the large x region in Fig. 2, few NuTeV data exist in such a region. It means that the $\varepsilon_v^{(1)}$ contribution to $sin^2\theta_W$ could be significantly reduced if the NuTeV kinematics is taken into account. The guideline of incorporating such experimental kinematics is supplied in Fig. 1 of Ref. [23]. The distribution ε_v could be effectively simulated by the NuTeV functions, $u_v^p - d_v^p$ and $d_v^p - u_v^p$, although physics motivation is completely different. Using the NuTeV functionals [23,24], we obtain the dashed curves in Fig. 3. Because of the lack of large x data, the contributions are significantly reduced.

The mechanism due to the nuclear modification difference between u_v and d_v could partially explain the NuTeV deviation, but it is not a major mechanism for the deviation according to Fig. 3. However, the distribution ε_v itself is not known at all, so that it would be too early to exclude the mechanism. On the other hand, it should be an interesting topic to investigate ε_v experimentally by the NuMI [20] and neutrino-factory [25] projects.

4. HERMES effect

The HERMES effect indicates nuclear modification of the longitudinal-transverse structure function ratio $R(x, Q^2)$. It was originally reported at small x ($0.01 < x < 0.03$) with small Q^2 ($0.5 < Q^2 < 1$ GeV^2) in the HERMES paper in 2000 [15]. There are theoretical investigations on this topic in terms of shadowing [26] and an isoscalar meson [27].

This interesting nuclear effect is, however, not observed in the CCFR/NuTeV experiments [17]. Although the CCFR/NuTeV target is the iron nucleus, observed R values agree well with theoretical calculations for the nucleon in the same kinematical region with the HERMES. Furthermore, a more careful HERMES analysis of radiative corrections showed such modification does not exist anymore [18].

Considering these experimental results, one may think that such a nuclear effect does not exist at all. However, we point out that the effect should exist in a different kinematical region, namely at large x with small Q^2 [16]. The ex-

istence of a nuclear effect in $R(x,Q^2)$ is important not only for investigating nuclear structure in the parton model but also for many analyses of lepton scattering data. For example, the SLAC parametrization in 1990 [28] has been used as a popular one. However, the data contain nuclear ones, so that one cannot use it for nucleon scattering studies if large nuclear effects exist in the data. Because of the importance of $R(x,Q^2)$ in lepton scattering analyses, we investigate the possibility of nuclear modification theoretically.

The structure function for the photon polarization λ is $W_\lambda^{A,N} = \varepsilon_\lambda^{\mu *}\,\varepsilon_\lambda^\nu\, W_{\mu\nu}^{A,N}$, so that longitudinal and transverse ones are defined by $W_T^{A,N} = (W_{+1}^{A,N} + W_{-1}^{A,N})/2$ and $W_L^{A,N} = W_0^{A,N}$. Here, N and A denote the nucleon and a nucleus, respectively. Lepton-hadron scattering cross section is described by a lepton tensor multiplied by a hadron tensor $W_{\mu\nu}$. In the electron scattering, the tensors for the nucleon and a nucleus are given by

$$W_{\mu\nu}^{A,N}(p_{_{A,N}},q) = -W_1^{A,N}(p_{_{A,N}},q)\left(g_{\mu\nu} - \frac{q_\mu q_\nu}{q^2}\right) + W_2^{A,N}(p_{_{A,N}},q)\,\frac{\widetilde{p}_{_{A,N}\mu}\,\widetilde{p}_{_{A,N}\nu}}{p_{_{A,N}}^2}\ , \quad (13)$$

where $\widetilde{p}_\mu = p_\mu - (p\cdot q)\,q_\mu/q^2$. In terms of these structure functions, the longitudinal and transverse structure functions are given $W_T^{A,N} = W_1^{A,N}$ and $W_L^{A,N} = (1+\nu_{_{A,N}}^2/Q^2)W_2^{A,N} - W_1^{A,N}$ by taking the nucleus or nucleon rest frame. Here, $\nu_A \equiv \nu$, and the photon momentum in the nucleon rest frame is denoted $(\nu_N, \vec{q}_N)$ with $\nu_N^2 = (p_N\cdot q)^2/p_N^2$.

We use a conventional convolution description for nuclear structure functions:

$$W_{\mu\nu}^A(p_A,q) = \int d^4p_N\, S(p_N)\, W_{\mu\nu}^N(p_N,q)\ , \quad (14)$$

where p_N is the nucleon momentum and $S(p_N)$ is the spectral function which indicates the nucleon momentum distribution in a nucleus. In order to investigate the longitudinal and transverse components, we introduce projection operators which satisfy $\widehat{P}_1^{\mu\nu}W_{\mu\nu}^A = W_1^A$ and $\widehat{P}_2^{\mu\nu}W_{\mu\nu}^A = W_2^A$. They are explicitly written as $\widehat{P}_1^{\mu\nu} = -(1/2)\left(g^{\mu\nu} - \widetilde{p}_A^\mu\,\widetilde{p}_A^\nu/\widetilde{p}_A^2\right)$ and $\widehat{P}_2^{\mu\nu} = -p_A^2/(2\,\widetilde{p}_A^2)\left(g^{\mu\nu} - 3\,\widetilde{p}_A^\mu\,\widetilde{p}_A^\nu/\widetilde{p}_A^2\right)$. Instead of W_1 and W_2 structure functions, the functions F_1 and F_2 are usually used: $F_1^{A,N} = \sqrt{p_{_{A,N}}^2}\,W_1^{A,N}$ and $F_2^{A,N} = (p_{_{A,N}}\cdot q/\sqrt{p_{_{A,N}}^2})\,W_2^{A,N}$. Then, the longitudinal structure function is given by

$$F_L^{A,N}(x_{_{A,N}},Q^2) = \left(1+\frac{Q^2}{\nu_{_{A,N}}^2}\right)F_2^{A,N}(x_{_{A,N}},Q^2) - 2x_{_{A,N}}F_1^{A,N}(x_{_{A,N}},Q^2)\,, \quad (15)$$

where $x_A = Q^2/(2\,p_A\cdot q)$ and $x_N = Q^2/(2\,p_N\cdot q)$. The ratio R_A of the longitudinal cross section to the transverse one is expressed by the function $R_A(x_A,Q^2)$:

$$R_A(x_A,Q^2) = \frac{F_L^A(x_A,Q^2)}{2\,x_A F_1^A(x_A,Q^2)}\ . \quad (16)$$

Applying the projection operators $\widehat{P}_1^{\mu\nu}$ and $\widehat{P}_2^{\mu\nu}$ to Eq. (14), we have

$$2\,x_A F_1^A(x_A,Q^2) = \int d^4\,p_N\,S(p_N)\,z\,\frac{M_N}{\sqrt{p_N^2}} \times\left[\left(1+\frac{\vec{p}_{N\perp}^{\,2}}{2\widetilde{p}_N^2}\right)2x_N F_1^N(x_N,Q^2) + \frac{\vec{p}_{N\perp}^{\,2}}{2\widetilde{p}_N^2}F_L^N(x_N,Q^2)\right], \quad (17)$$

$$F_L^A(x_A,Q^2) = \int d^4\,p_N\,S(p_N)\,z\,\frac{M_N}{\sqrt{p_N^2}} \times\left[\left(1+\frac{\vec{p}_{N\perp}^{\,2}}{\widetilde{p}_N^2}\right)F_L^N(x_N,Q^2) + \frac{\vec{p}_{N\perp}^{\,2}}{\widetilde{p}_N^2}2x_N F_1^N(x_N,Q^2)\right]. \quad (18)$$

These results are interesting. The transverse structure function for a nucleus is described not only by the transverse one for the nucleon but also by the longitudinal one with the admixture coefficient $\vec{p}_{N\perp}^{\,2}/(2\widetilde{p}_N^2)$. The $\vec{p}_{N\perp}$ is the nucleon momentum component perpendicular to the photon one $\vec{q}$. Equations (17) and (18) indicate that the transverse-longitudinal admixture exists because the nucleon momentum direction is not necessary along the virtual photon direction.

These expressions are numerically estimated for the nitrogen nucleus by taking a simple shell

model for the spectral function with density dependent Hartree-Fock wave functions. Parton distribution functions are taken from the MRST-1998 version and the nucleonic $R(x, Q^2)$ is taken from the SLAC analysis in 1990 [28]. The nitrogen-nucleon ratios $R_{^{14}N}/R_N$ are shown at Q^2=1, 10, 100 GeV^2 by the solid curves in Fig. 4. In order to clarify the admixture effects, the ratios are also calculated by suppressing the $\vec{p}^{\,2}_{N\perp}$ terms, and the results are shown by the dashed curves. In addition, the nuclear modification is calculated at Q^2=0.5 GeV^2 by using the GRV94 parametrization for the PDFs. It is intended to find the modification magnitude at smaller Q^2, where JLab experiments could possibly probe [29]. Because the admixture is proportional to $\vec{p}^{\,2}_{N\perp}/(2\widetilde{p}^{\,2}_N) \sim \vec{p}^{\,2}_{N\perp}/Q^2$, the modification effects are large at small Q^2 ($=0.5-1$ GeV^2) and they become small at large Q^2. However, the modification does not vanish even at Q^2=100 GeV^2 due to the Fermi-motion and binding effects which are contained implicitly in the spectral function.

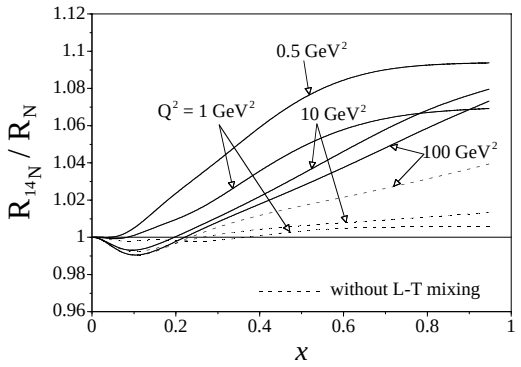

Figure 4. The nitrogen-nucleon ratio $R_{^{14}N}/R_N$ is shown at Q^2=0.5, 1, 10, and 100 GeV^2. The solid curves are the full results and the dashed ones are obtained by terminating the admixture effects.

In this way, we found that the nucleon Fermi motion, especially the perpendicular motion to the virtual photon direction, and the nuclear binding give rise to the nuclear modification of the longitudinal-transverse ratio $R(x, Q^2)$. However, nuclear modification of R in the large x region with small Q^2 has not been investigated experimentally. The situation is clearly illustrated in Fig. 3 of Ref. [17], where the data does not exist at $x = 0.5$ with $Q^2 \approx$1 GeV^2. We hope that future measurements, for example those of JLab experiments [29], are able to provide clear information on the nuclear modification in this region.

5. Summary

Current neutrino scattering experiments are done with nuclear targets, so that precise nuclear corrections should be taken into account in order to investigate underlying elementary processes, for example neutrino oscillation phenomena. In this paper, the discussions are focused on high-energy reactions.

First, the optimum nuclear parton distribution functions were determined by the χ^2 analysis of DIS and Drell-Yan data. They could be used for calculating high-energy nuclear cross sections.

Second, a possibility of explaining the NuTeV $sin^2\theta_W$ was investigated by the nuclear correction difference between u_v and d_v in the iron nucleus. Although the contribution to the $sin^2\theta_W$ deviation may not be large at this stage, the distribution $\varepsilon_v(x)$ should be investigated by future experiments.

Third, a possible HERMES-type effect was proposed in the medium and large x regions due to the nucleon Fermi motion and binding. Especially, we found that the perpendicular nucleon motion to the virtual photon direction gives rise to the admixture of longitudinal and transverse structure functions in the nucleon. Such an effect should be tested by electron and neutrino scattering experiments at large x with small Q^2.

Acknowledgments

S.K. was supported by the Grant-in-Aid for Scientific Research from the Japanese Ministry of Education, Culture, Sports, Science, and Technology. He thanks M. Sakuda for his financial support for participating in this workshop.

REFERENCES

1. http://nuint.ps.uci.edu.

2. M. Sakuda, http://nuint.ps.uci.edu/slides/Sakuda.pdf; in proceedings of this workshop.
3. E. A. Paschos and J. Y. Yu, Phys. Rev. D65 (2002) 033002.
4. Shi-yuan Li and Xin-Nian Wang, Phys. Lett. B527 (2002) 85; X. Zhang and G. Fai, Phys. Rev. C65 (2002) 064901; A. Chamblin and G. C. Nayak, Phys. Rev. D66 (2002) 091901.
5. B. Z. Kopeliovich and A. V. Tarasov, Nucl. Phys. A710 (2002) 180; L. Frankfurt, V. Guzey, and M. Strikman, hep-ph/0303022; N. Armesto *et. al.*, hep-ph/0304119.
6. http://durpdg.dur.ac.uk/hepdata/pdf.html.
7. K. J. Eskola, V. J. Kolhinen, and P. V. Ruuskanen, Nucl. Phys. B535 (1998) 351; K. J. Eskola, V. J. Kolhinen, and C. A. Salgado, Eur. Phys. J. C9 (1999) 61.
8. M. Hirai, S. Kumano, and M. Miyama, Phys. Rev. D64 (2001) 034003; research in progress. See http://hs.phys.saga-u.ac.jp/nuclp.html.
9. G. P. Zeller *et. al.*, Phys. Rev. Lett. 88 (2002) 091802.
10. K. S. McFarland *et. al.*, Nucl. Phys. B 112 (2002) 226.
11. G. A. Miller and A. W. Thomas, hep-ex/0204007; G. P. Zeller *et. al.*, hep-ex/0207052. W. Melnitchouk and A. W. Thomas, Phys. Rev. C67 (2003) 038201; S. Kovalenko, I. Schmidt, and J.-J. Yang, Phys. Lett. B546 (2002) 68.
12. S. Kumano, Phys. Rev. D66 (2002) 111301.
13. S. A. Kulagin, Phys. Rev. D67 (2003) 091301.
14. S. Davidson *et. al.*, J. High Energy Phys. 0202, 037 (2002); E. Ma and D. P. Roy, Phys. Rev. D65 (2002) 075021; C. Giunti and M. Laveder, hep-ph/0202152; W. Loinaz, N. Okamura, T. Takeuchi, and L. C. R. Wijewardhana, Phys. Rev. D67 (2003) 073012.
15. K. Ackerstaff *et al.*, Phys. Lett. B475 (2000) 386.
16. M. Ericson and S. Kumano, Phys. Rev. C 67 (2003) 022201.
17. U. K. Yang *et al.*, Phys. Rev. Lett. 87 (2001) 251802.
18. A. Airapetian *et al.*, hep-ex/0210067 & 0210068.
19. S. Kumano, Phys. Rep. 303 (1998) 183; G. T. Garvey and J.-C. Peng, Prog. Part. Nucl. Phys. 47 (2001) 203.
20. J. G. Morfin, Nucl. Phys. B112 (2002) 251.
21. D. Abbaneo *et. al.*, hep-ex/0112021. See also the reference [21] in Ref. [9].
22. E. A. Paschos and L. Wolfenstein, Phys. Rev. D7 (1973) 91.
23. G. P. Zeller *et. al.*, Phys. Rev. D65 (2002) 111103 .
24. K. S. McFarland and G. P. Zeller, personal communications.
25. http://www.cap.bnl.gov/nufact03/.
26. V. Barone and M. Genovese, hep-ph/9610206; B. Kopeliovich, J. Raufeisen, and A. Tarasov, Phys. Rev. C62 (2000) 035204.
27. G. A. Miller, S. J. Brodsky, and M. Karliner, Phys. Lett. B481 (2000) 245; G. A. Miller, Phys. Rev. C64 (2001) 022201.
28. L. W. Whitlow, S. Rock, A. Bodek, S. Dasu, and E. M. Riordan, Phys. Lett. B250 (1990) 193; L. W. Whitlow, report SLAC-357 (1990).
29. H. P. Blok, personal communications. A. Brüll *et al.*, http://www.jlab.org/exp_prog /proposals/99/PR99-118.pdf.